Characteristics of Undamaged Asphalt Mixtures in Tension and Compression[1]

Robert L. Lytton, Ph.D., P.E.
Professor, Fred J. Benson Chair
Zachry Department of Civil Engineering
Texas A&M University
3136 TAMU, CE/TTI Bldg. 503A, College Station, Texas 77843
Phone: (979) 845-9964, Email: r-lytton@civil.tamu.edu

Fan Gu, Ph.D.
Postdoctoral Researcher
National Center for Asphalt Technology
Auburn University
277 Technology Parkway, Auburn, AL 36830
Phone: (334)-844-6251, Email: fzg0014@auburn.edu

Yuqing Zhang, Ph.D.
Lecturer
School of Engineering and Applied Science
Aston University
MB153A, Aston Triangle, Birmingham, B4 7ET, U.K.
Phone: +44 (0) 121-204-3391, Email: y.zhang10@aston.ac.uk

Xue Luo, Ph.D.
Assistant Research Scientist
Texas A&M Transportation Institute
Texas A&M University System
3135 TAMU, CE/TTI Bldg. 508B, College Station, Texas 77843
Phone: (979) 458-8535, Email: rongluo@tamu.edu

[1] This is an Accepted Manuscript of an article published by *International Journal of Pavement Engineering*. The published article is available at http://dx.doi.org/10.1080/10298436.2017.1279489

Abstract

Cracking in asphalt pavements is the net result of fracture and healing. Healing is the anti-fracture. The ability to accurately measure and predict the appearance of cracking depends on being able to determine the material properties of an asphalt mixture that govern the rate of development of these two contrary aspects of cracking.

This study is devoted to identifying the datum material properties in undamaged samples. It will make use of viscoelastic formulations and of well-known mechanics concepts the way in which these properties are altered by the composition of the mixture. Also introduced in this study is a process that makes extensive use of the pseudo-strain concept in decomposing the strain components when damage occurs into the non-linear elastic, plastic, viscoplastic, and viscofracture strains. One of the many benefits of this approach is the ability to measure the fatigue endurance limit of an asphalt mixture with a simple test that requires only half an hour.

The study begins with a detailed discussion of these concepts and properties and the test methods that simply and accurately measure them. One of the great advantages of using mechanics is that it provides a rapid and efficient way to predict the rate of appearance of the two aspects of pavement cracking, fracture and healing. Mechanics requires the use of material properties. An accurate and efficient determination of undamaged material properties is fundamental and important to the prediction of the performance of asphalt mixtures. It is found that the undamaged properties of an asphalt mixture are different when they are loaded in tension or in compression and this distinction is important.

This study addresses the efficiency of the laboratory testing methods, and the effects of the volumetric material components and environmental factors such as temperature and aging on the undamaged material properties. It also introduces the non-destructive tests that must be made in order, subsequently, to measure the damaged properties of the same materials which are the subject of the second study.

Keywords: asphalt mixtures; viscoelasticity; complex modulus; master curve; anisotropy; pseudostrain energy; strain decomposition; modulus gradient; aging.

1. Background

Cracking in asphalt pavements is a practical problem with several dimensions. When it appears in existing pavements, it is difficult and costly to correct, especially if it occurs before it was expected. Whether the timing of its appearance is due to the level of construction quality or to the original design of the composition of the mixture or to environmental or traffic intensity influences is an important question that needs to be answered correctly because of the very large annual budgets that are expended on the construction, maintenance and rehabilitation of such pavements. In addition, the effects on this very destructive distress of using recycled materials is another major question that must be answered correctly if the cost of pavement cracking can be reduced by practical actions within the design, build, maintain and rehabilitate chain.

This is the motivation for research into cracking in asphalt pavements. Two principal approaches have been and continue to be used in this research: (1) the "simulate and correlate" approach and (2) the "cause and effect" approach. The first approach will show immediate results if the number of relevant factors is fairly small. However as the number of factors increases, the size of the factorial experiments to identify the most sensitive factors gets out of control quickly. The second approach relies mainly upon the use of mechanics which itself relies on the identification and measurement of material properties which can be measured directly and used for the design of the composition of the mixture and for construction specifications. The environmental and traffic intensity effects can be accounted for directly by carefully designed and simply conducted tests of the material properties in the laboratory and the field. This approach is easily adaptable to using computer modeling to predict the future cracking performance and reliability of the mixture once it is built. Reliability depends upon the as-built variability of the mixture which is a natural outcome of the construction process and can be easily incorporated in the second approach.

The use of mechanics requires that the material is properly characterized. If it is viscoelastic, viscoelastic properties must be measured and used. If it undergoes plastic deformation, it must make use of viscoplastic material properties. Cracking in asphalt mixtures is no different. Cracking is the net result of fracture and healing, and there are material properties of asphalt mixtures that are relevant to both processes. The mechanics representation of the relevant properties in both fracture and healing must start with the datum state: the undamaged properties. Both fracture and healing result in a change in the response of the damaged material to applied stresses, whether applied by traffic or changes in thermal or moisture stresses. A fractured material will be softer, more

compliant and weaker than it was in its undamaged state, but its fundamental fracture material properties will not have changed. Material properties will change due to aging or to the intrusion of moisture into the components of the mixture or onto the interfaces between them. A similar statement can be made about the healing properties.

A material property is independent of the dimensions or geometry of the specimen which is tested to determine that property. Recognition of this fact is an advantage because it allows the use of samples that are easier to form and to test to determine those material properties. The simplicity of the sample makes the measured data much easier to reduce and to interpret and allows the testing results to be both more accurate and less costly in time and testing equipment.

Prediction of damage depends upon what is understood as "damage". There are two types of "damage" that are commonly predicted. One of these is an imputed damage and the other is an actual physical damage. Imputed damage is inferred from a measured departure from a linear viscoelastic response of a material to some applied stress. The actual physical damage is the type of damage that is the subject of fracture and healing. It means the predicted loss of cross sectional area because of the growth of a crack or multiple cracks.

This first study is devoted to identifying the datum material properties in undamaged samples. It will make use of viscoelastic formulations and of well-known mechanics concepts such as the elastic-viscoelastic correspondence principle, the concept of pseudostrain, the time-temperature shift function and the way in which these properties are altered by the composition of the mixture. Also introduced in this study is a process that makes extensive use of the pseudo-strain concept in decomposing the strain components when damage occurs into the non-linear elastic, plastic, viscoplastic, and viscofracture strains. One of the many benefits of this approach is the ability to measure the fatigue endurance limit of an asphalt mixture with a simple test that requires only a few minutes.

The second study is devoted to the determination of the material properties that govern the appearance of plastic, viscoplastic and viscofracture strains and healing and how these damage properties are altered by aging, moisture, and the time-temperature shift. It also demonstrates how these properties are measured in samples formed in the laboratory and taken as cores in the field.

Fracture and healing are the fundamental mechanisms of fatigue cracking in pavements as well as the other types of cracking that affect pavement performance: thermal cracking, longitudinal cracking, and reflection cracking. An understanding of the fundamental properties of an asphalt

mixture that govern the appearance of all of these types of cracking provide a list of the properties that can be altered by design to extend the cracking lives of these asphalt pavements.

2. Introduction to Mechanics Terminology

Asphalt mixtures are known to be time and frequency dependent, and exhibit as a viscoelastic material in undamaged conditions. The viscoelastic deformation of an asphalt mixture is recoverable and does not contribute to the permanent deformation of the material. However, to characterize the performance of damaged asphalt mixtures, it is required to accurately measure the viscoelastic responses for the undamaged asphalt mixtures and eliminate them from the total responses in damaged conditions.

The viscoelastic properties of asphalt mixtures include relaxation modulus and time-dependent Poisson's ratio in the time domain and complex modulus and complex Poisson's ratio in the frequency domain. These variables are anisotropic and interconvertible between the time and frequency domains. The time, frequency and temperature dependence of these complex material properties are characterized by master curves of the magnitudes and phase angles. It is critical to be able to differentiate between the properties of the undamaged and damaged asphalt mixtures, which can be observed directly with simple tests that vary the loading time or loading cycles. Based on the accurate determination of the material properties of undamaged asphalt mixtures, the responses of damaged asphalt mixtures can be decomposed into viscoelastic, viscoplastic and viscofracture components based on the Elastic-Viscoelastic Correspondence Principle (EVCP) developed by Schapery (1984) together with a three dimensional EVCP developed by the authors (Zhang et al. 2014c). The decomposed individual strains can then be employed for effective damage modeling and characterization including permanent deformation and fracture.

An accurate and efficient determination of undamaged material properties is fundamental and important to the prediction of the performance of asphalt mixtures. This should also address the efficiency of laboratory testing methods, and the effect of volumetric material components, and environmental factors such as temperature and aging on these material properties.

3. Linear Viscoelastic Constitutive Relations for Undamaged Asphalt Mixtures

3.1 Uniaxial Condition

Based on the viscoelastic theories, in uniaxial condition, the axial strain and stress can be related as follows (Wineman and Rajagopal, 2001):

$$\begin{cases} \varepsilon_1(t) = \int_{0^-}^{t} D(t-\tau) d\sigma_1(\tau) \\ \sigma_1(t) = \int_{0^-}^{t} E(t-\tau) d\varepsilon_1(\tau) \end{cases} \quad (1)$$

where $\varepsilon_1(t)$ is axial strain; $\sigma_1(t)$ is the axial stress; $D(t)$ is creep compliance; $E(t)$ is relaxation modulus; t is current time; and τ is a integration variable that is less than or equal to t. Taking the Laplace transform of Equation 1 gives a relationship between the creep compliance and the relaxation modulus (Findley, et al., 1989):

$$\bar{E}(s)\bar{D}(s) = \frac{1}{s^2} \quad (2)$$

where $\bar{E}(s)$ and $\bar{D}(s)$ are the Laplace transforms of $E(t)$ and $D(t)$, respectively; and s is a variable in the Laplace domain.

To determine the radial strain, the time-dependent Poisson's ratio ($\upsilon_{12}(t)$) is employed as an important material property in the model in Equation 3. For the purpose of strain decomposition, a new viscoelastic variable that is named as the Pi-son's ratio ($\pi_{12}(t)$) is proposed (Zhang et al. 2014c). The viscoelastic Poisson's ratio and Pi-son's ratio are defined as:

$$\begin{cases} \varepsilon_2(t) = -\int_{0^-}^{t} \upsilon_{12}(t-\tau) d\varepsilon_1(\tau) \\ \varepsilon_1(t) = -\int_{0^-}^{t} \pi_{12}(t-\tau) d\varepsilon_2(\tau) \end{cases} \quad (3)$$

where $\varepsilon_1(t)$ is axial strain; and $\varepsilon_2(t)$ is radial strain; $\upsilon_{12}(t)$ is viscoelastic Poisson's ratio; $\pi_{12}(t)$ is viscoelastic Pi-son's ratio. A relationship between $\upsilon_{12}(t)$ and $\pi_{12}(t)$ can be derived as.

$$\bar{\pi}_{12}(s)\bar{\upsilon}_{12}(s) = \frac{1}{s^2} \quad (4)$$

where $\bar{\upsilon}_{12}(s)$ and $\bar{\pi}_{12}(s)$ are the Laplace transforms of $\upsilon_{12}(t)$ and $\pi_{12}(t)$, respectively.

3.2 Multi-axial Conditions

Under multi-axial stress states, the isotropic constitutive relation for an undamaged linear viscoelastic material is expressed as:

$$\sigma_{ij} = \frac{1}{3}\sigma_{kk}\delta_{ij} + s_{ij} = \delta_{ij}\int_0^t K(t-\tau)\frac{\partial \varepsilon_{kk}^{ve}}{\partial \tau} d\tau + 2\int_0^t G(t-\tau)\frac{\partial e_{ij}^{ve}}{\partial \tau} d\tau \quad (5)$$

where $\sigma_{kk} = \sigma_{11} + \sigma_{22} + \sigma_{33}$ is the volumetric stress, $\varepsilon_{kk}^{ve} = \varepsilon_{11}^{ve} + \varepsilon_{22}^{ve} + \varepsilon_{33}^{ve}$ = viscoelastic volumetric strain, $K(t)$ = relaxation bulk modulus, $s_{ij} = \sigma_{ij} - 1/3\,\sigma_{kk}\delta_{ij}$ = deviatoric stress tensor and δ_{ij} = the *Kronecker* delta, $e_{ij}^{ve} = \varepsilon_{ij}^{ve} - 1/3\,\varepsilon_{kk}^{ve}\delta_{ij}$ = viscoelastic deviatoric strain, $G(t)$ = relaxation shear modulus, t = a current time of interest, and τ = an integration variable. Note that in Eq.5., a 've' was used in the superscript to emphasize that this is a viscoelastic strain. It equals to total strain in undamaged condition whereas it's a portion of total strain in the damage conditions.

Relationships between material properties can be formulated in the Laplace domain as:

$$\begin{cases} s\bar{G}(s) = \dfrac{s\bar{E}(s)}{2\left[1 + s\bar{\upsilon}_{12}(s)\right]} \\ s\bar{K}(s) = \dfrac{s\bar{E}(s)}{3\left[1 - 2s\bar{\upsilon}_{12}(s)\right]} \end{cases} \tag{6}$$

If a solid-like generalized Maxwell (Prony) model is used, the total stress becomes:

$$\sigma_{ij} = K_{\infty}\varepsilon_{kk}^{ve}\delta_{ij} + 2G_{\infty}e_{ij}^{ve} + \sum_{m=1}^{M}\left[K_m\left(\varepsilon_{kk}^{ve} - \varepsilon_{kk}^{m\cdot vi}\right)\delta_{ij} + 2G_m\left(e_{ij}^{ve} - e_{ij}^{m\cdot vi}\right)\right] \tag{7}$$

where M = total number of the Maxwell elements. K_∞ and G_∞ are the long term equilibrium bulk modulus and shear modulus, respectively; K_m and G_m are components of the relaxation bulk and shear moduli respectively; $\varepsilon_{kk}^{m\cdot vi}$ and $e_{ij}^{m\cdot vi}$ are the viscous bulk and deviatoric strains caused by the m-th dashpot (m = 1,2,…, M) in the generalized Maxwell model, which are solved by:

$$\begin{cases} \left(a_T\tau_m\right)\dot{\varepsilon}_{kk}^{m\cdot vi} + \varepsilon_{kk}^{m\cdot vi} - \varepsilon_{kk}^{ve} = 0 \\ \left(a_T\tau_m\right)\dot{e}_{ij}^{m\cdot vi} + e_{ij}^{m\cdot vi} - e_{ij}^{ve} = 0 \end{cases} \tag{8}$$

where τ_m = relaxation time for the m-th dashpot at a reference temperature, and a_T = time-temperature shift factor for the modulus, that can be modelled by the Arrhenius function in Equation 9.

$$a_T(T) = \exp\left[\frac{\Delta E}{R}\left(\frac{1}{T} - \frac{1}{T_r}\right)\right] \tag{9}$$

where ΔE = activation energy for the temperature effect on modulus, R = universal gas constant, 8.314 $J/(K{\cdot}mol)$. T = temperature of interest, T_r = reference temperature.

4. Time, Frequency, and Temperature Dependence of Asphalt Mixture Properties

4.1 Determination of Damaged and Undamaged Condition

The undamaged and damaged conditions of asphalt mixtures can be differentiated based on the variation of viscoelastic material properties, namely the complex modulus and phase angle. In undamaged conditions (low stress or strain levels), the viscoelastic material properties remain unchanged with loading time or cycles; whereas in damaged conditions (high stress or strain levels), they vary with loading time or cycles. The undamaged conditions consist of two stages: linear viscoelastic region and nonlinear viscoelastic (without damage) region (Luo et al. 2013b). The threshold between the undamaged and damaged conditions is defined as the critical nonlinear viscoelastic state. The material properties are different in compression and in tension.

In compression, at a low stress level, e.g., 70 kPa in Figure 1 showing the dynamic moduli and phase angles at every 10 load cycles intervals for an asphalt mixture, the dynamic modulus and phase angle remain constant as the load cycles increase, which indicates that the sample is tested in an undamaged condition.

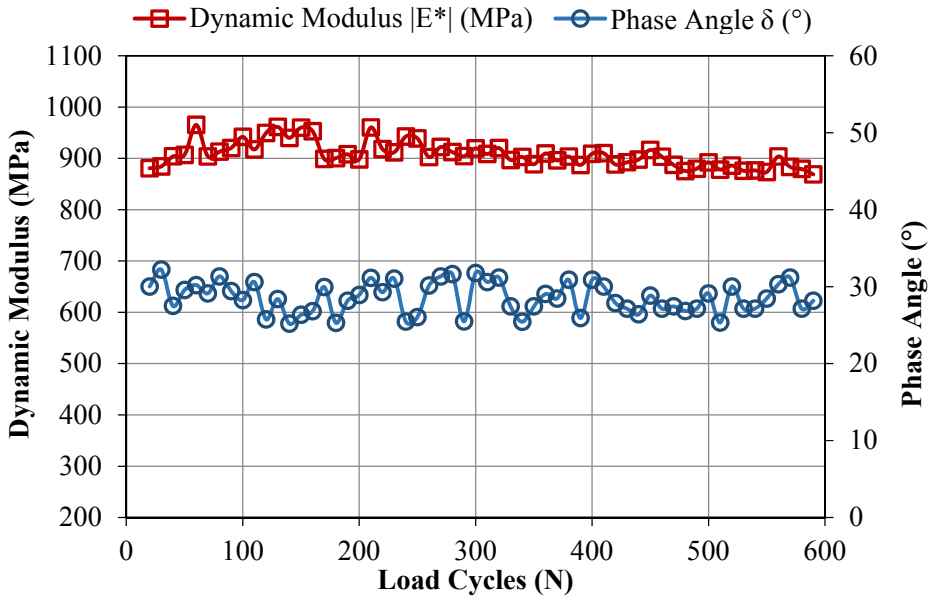

Figure 1. Dynamic modulus and phase angle of an undamaged asphalt mixture at 40°C

In compression, at a high stress level, e.g., 600 kPa in Figure 2 showing the dynamic modulus and phase angle of a damaged asphalt mixture at 10 load cycle intervals, the viscoelastic responses become time (or load cycle)-dependent at a constant loading frequency. The damaged compressive response has three phases: (I) increasing stiffness and decreasing phase angle; (II)

slight decline of stiffness and constant phase angle, and (III) sharp decline of stiffness and increase of phase angle. Detailed interpretation of Figure 2 can be found in Zhang (2012a).

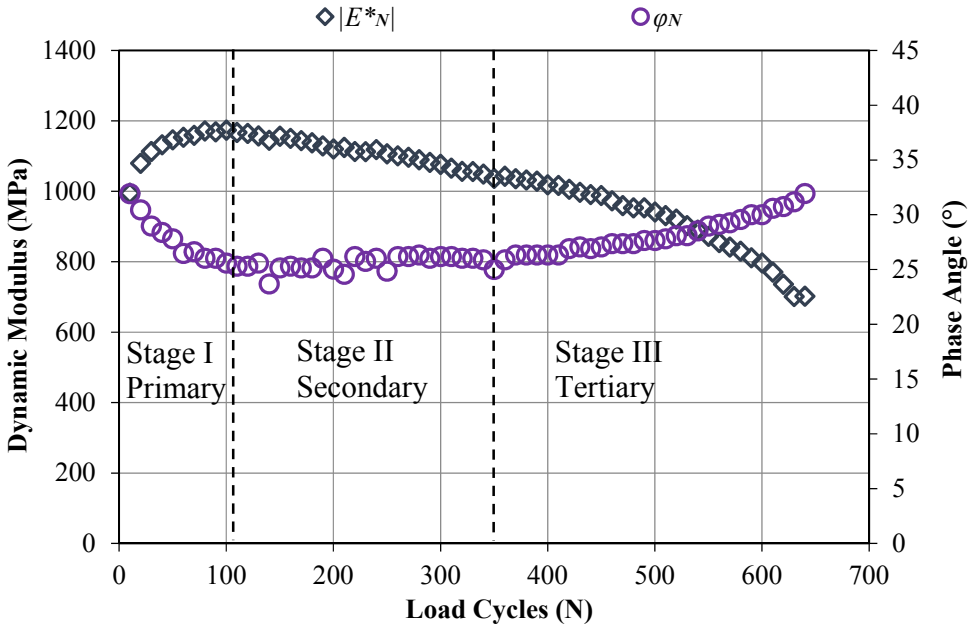

Figure 2. Dynamic modulus and phase angle of a damaged asphalt mixture at 40°C

Incremental stress or strain steps in dynamic modulus tests can be employed to determine the critical stress or strain level for the separation of undamaged and damaged asphalt mixtures, as that has done in Figures 1 and 2. Linear viscoelasticity is hypothesized for an undamaged asphalt mixture in compression and any nonlinearity is due to the irrecoverable plastic, viscoplastic, or viscofracture deformation.

In tension, the dynamic moduli and phase angles of asphalt mixtures at a low strain level (e.g., 40 με) also remain unchanged as the load cycles increase, as shown in Figure 3a. This demonstrates that the tension test at such a low strain level is a non-destructive test. Figure 3b presents the evolution of dynamic moduli and phase angles with the number of load cycles at a high strain level (e.g., 200 με). The measured dynamic moduli decrease, while the measured phase angles increase with increasing load cycles. The tension test at such a high strain level damages the tested asphalt mixtures. The viscoelastic responses of the damaged asphalt mixtures vary with the number of load cycles in the destructive tension test (Luo et al. 2013a).

The controlled-strain repeated direct tension (RDT) tests at incremental strain levels are capable of determining the fatigue endurance limit of asphalt mixtures (Luo et al. 2013b, 2014a). Other endurance limit tests include the traditional beam fatigue test and uniaxial repeated load test

(Carpenter et al. 2003; Witczak et al. 2013). The controlled-strain RDT test protocol requires much shorter time due to the application of the critical nonlinear viscoelastic definition and the features of the material properties demonstrated above.

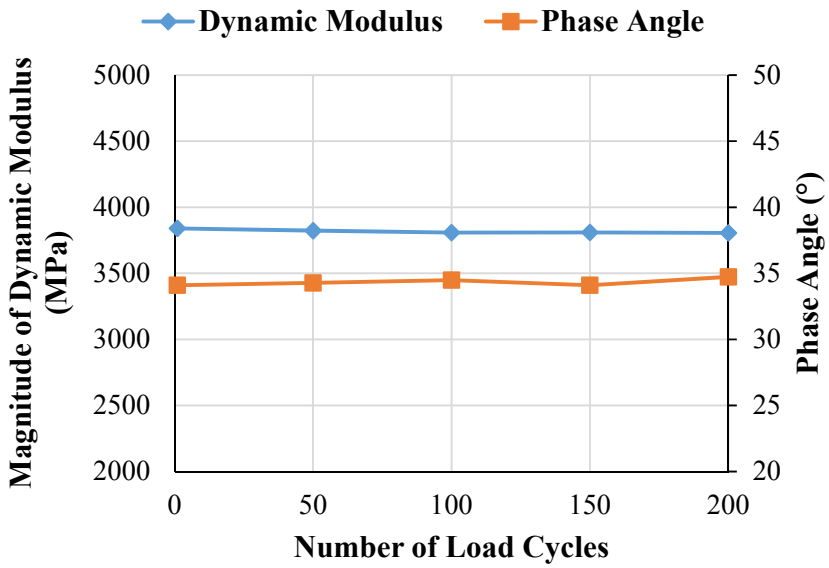

a. Tensile dynamic modulus and phase angle of an undamaged asphalt mixture at 20°C

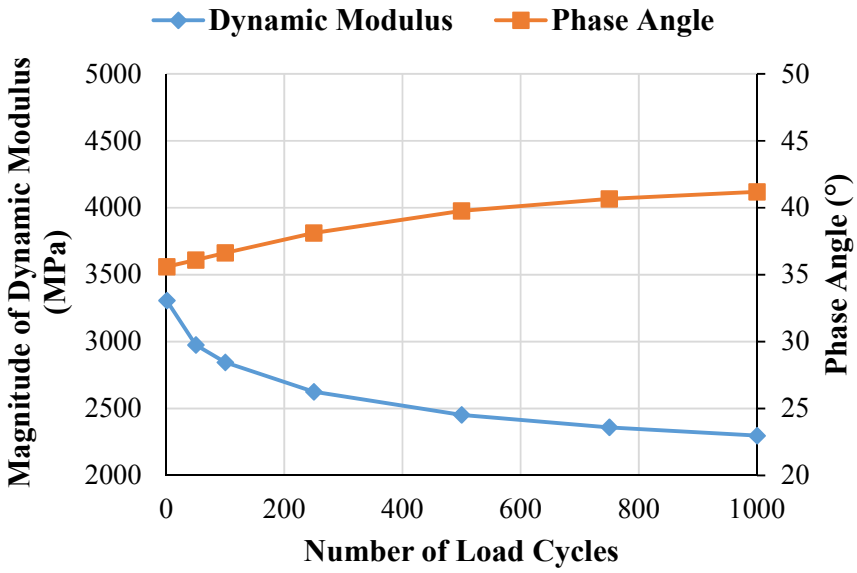

b. Tensile dynamic modulus and phase angle of a damaged asphalt mixture at 20°C

Figure 3. Evolution of dynamic moduli and phase angles of asphalt mixture with the number of load cycles

4.2 Master Curves of Asphalt Mixtures

The master curves of the complex modulus and phase angle are two important undamaged properties of asphalt mixture. They are used to predict the viscoelastic behavior of asphalt mixture over a wide frequency and temperature range. The master curves for the magnitude of complex modulus and complex Poisson's ratio are recommended to use Christensen-Anderson-Marasteanu (CAM) models (Marasteanu and Anderson 1999) as in below:

$$\left|E^*(\omega)\right| = \frac{E_g}{\left[1+\left(\frac{\omega_{cE}}{\omega \cdot 10^{C_E(T-T_r)}}\right)^{\frac{\log 2}{R_E}}\right]^{\frac{R_E}{\log 2}}} \tag{10}$$

where E_g = glassy modulus of the asphalt mixture, MPa; ω_{cE} = crossover frequency of the asphalt mixture for modulus, rad/sec; R_E = rheological index of the asphalt mixture for modulus; and C_E = slope of the time-temperature shift factor for modulus. The CAM model in Equation 10 yields a rising "S-shaped" curve for the magnitude of the complex modulus that approaches the horizontal glassy modulus of an asphalt mixture at an asymptote of E_g. An example of a master curve of the magnitude of the complex modulus (i.e., dynamic modulus) is shown in Figure 4. The complex Poisson's ratio is given by Equation 11:

$$\left|\nu^*(\omega)\right| = \frac{\nu_g}{\left[1+\left(\frac{\omega \cdot 10^{C_\nu(T-T_r)}}{\omega_{c\nu}}\right)^{\frac{\log 2}{R_\nu}}\right]^{\frac{R_\nu}{\log 2}}} \tag{11}$$

where ν_g = glassy Poisson's ratio of the asphalt mixture; $\omega_{c\nu}$ = crossover frequency of the asphalt mixture for Poisson's ratio, rad/sec; R_ν = rheological index for Poisson's ratio; and C_ν = slope of the time-temperature shift factor for Poisson's ratio. The magnitude of the complex Poisson's ratio decreases as the frequency increases, thus the master curve for the complex Poisson's ratio magnitude shows a falling S-shaped curve on the frequency domain.

A β-model (Zhang et al. 2012b) is proposed for the phase angle master curve of both complex modulus and complex Poisson's ratio. This model produces a non-symmetric bell-shaped curve on the plot of phase angle versus the logarithm of frequency.

$$\varphi = \frac{\varphi_{max}}{Exp\left\{\left(\frac{\beta+1}{\beta}\right)\left[\left(\frac{\omega_R}{\omega\cdot\alpha_T}\right)^{\beta}-1\right]\right\}\left(\frac{\omega\cdot\alpha_T}{\omega_R}\right)^{\beta+1}} \quad (12)$$

where φ_{max} = the maximum phase angle, degrees; ω_R = the reference frequency where φ_{mE} occurs, rad/sec. β = a parameter that determines the curvature of the phase angle master curve; α_T = time-temperature shift factor. α_T = time-temperature shift function, for which the Arrhenius function in Equation 9 is recommended. When $\varphi_{max} > 0$, it produces a bell-shaped curve function for the master curve of the phase angle of the complex modulus; while when $\varphi_{max} < 0$, it yields an inverted bell-shaped curve function for the master curve of the phase angle of the complex Poisson's ratio. An example master curve for the phase angle of the complex modulus is shown in Figure 5.

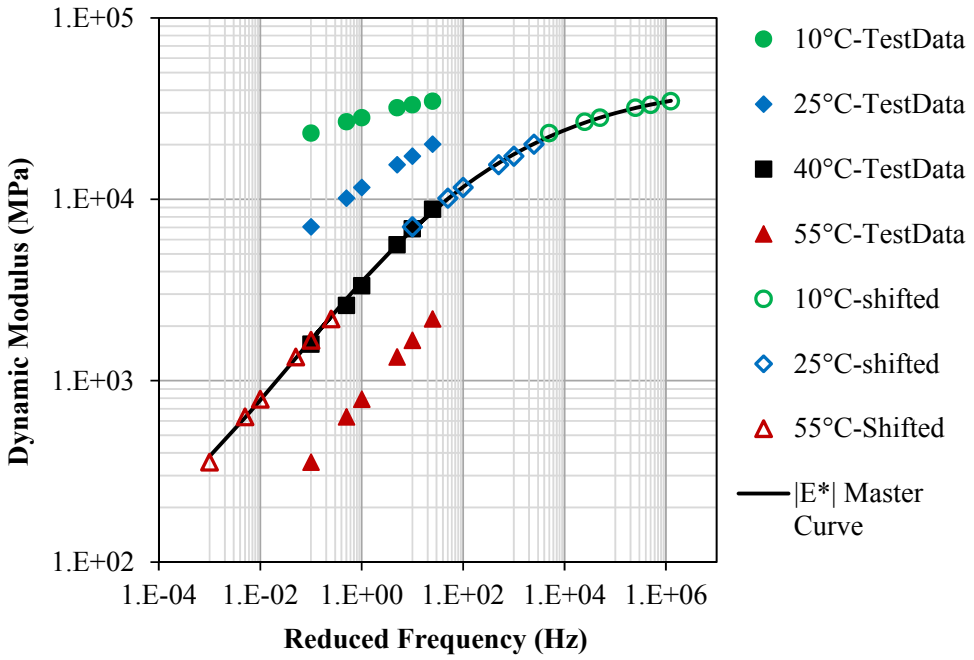

Figure 4. Dynamic modulus master curve for an asphalt mixture at 40°C in compression

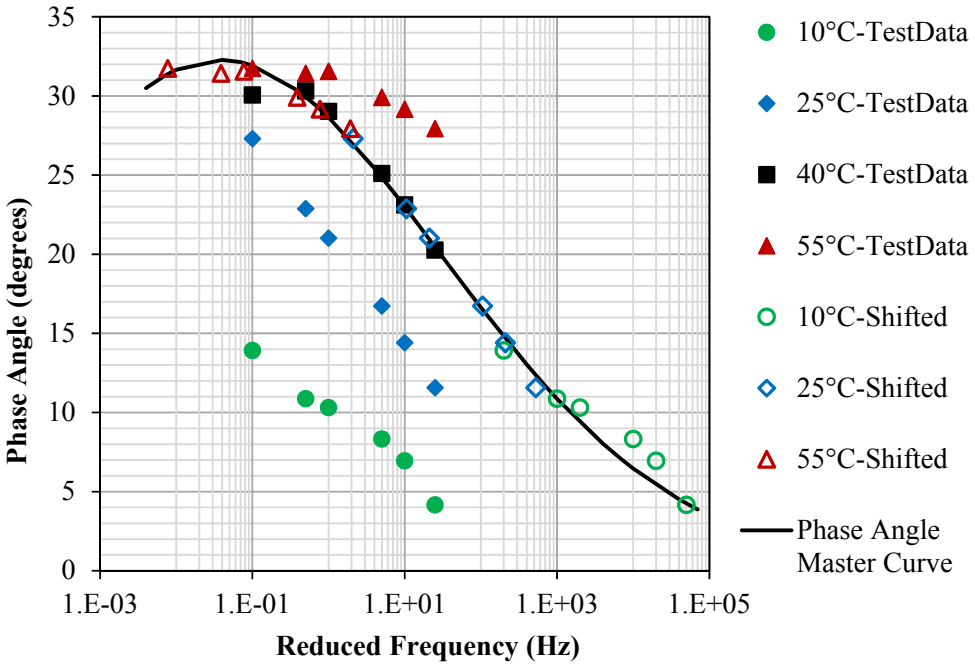

Figure 5. Phase angle master curve for an asphalt mixture at 40°C in compression

The traditional dynamic modulus test is used to determine the undamaged properties of asphalt mixture in compression. However, asphalt mixtures exhibit different viscoelastic behavior in compression and in tension (Luo et al. 2013a). Thus, the tensile viscoelastic properties (i.e., tensile dynamic modulus and phase angle) are also determined to fully characterize the viscoelastic behavior of an asphalt mixture. Previous studies (Si 2001; Arambula 2007; Gu et al. 2015a and 2015b) show that the tensile viscoelastic properties are usually determined by applying a repeated tensile load or a uniaxial tensile load with a controlled strain level to the test specimen. These test methods are time-consuming to complete a sizable factorial design with multiple test temperatures and frequencies. An alternative method measures the tensile dynamic modulus and phase angle of asphalt mixture, by applying a uniaxial monotonically increasing tensile stress to the test specimen. The test is performed non-destructively on the same specimen at three temperatures (i.e., 10°C, 20°C, and 30°C). The relaxation modulus is calculated by applying the inverse Laplace transform, which is shown in Equation 13.

$$E(t) = L^{-1}\left\{\frac{\bar{\sigma}(s)}{s\bar{\varepsilon}(s)}\right\} \tag{13}$$

where $E(t)$ is the relaxation modulus as a function of time t, L^{-1} represents the inverse Laplace transform, $\bar{\sigma}(s)$ is the Laplace transform of the time-dependent stress, and $\bar{\varepsilon}(s)$ is the Laplace transform of the time-dependent strain. Knowing the relaxation modulus, the tensile complex modulus is obtained using Equation 14 (Park and Schapery 1999).

$$E^*(\omega) = i\omega L\{E(t)\}_{s=i\omega} \tag{14}$$

where $E^*(\omega)$ is the tensile complex modulus as a complex function of frequency, and L represents the Laplace transform. Then the real part and imaginary part of the tensile complex modulus can be obtained from Equation 14. The phase angle can be determined by dividing the imaginary part of $E^*(\omega)$ by the real part of $E^*(\omega)$. The master curves of the magnitude and phase angle of the tensile complex modulus are constructed using the time-temperature superposition principle. The details of the data analysis and master curve construction procedure can be found in Luo and Lytton (2010).

4.3 Correspondence Principles

Schapery (1984) developed elastic-viscoelastic correspondence principle (EVCP) and found that, if the actual strain is replaced by a pseudostrain, the constitutive equation for a viscoelastic material is identical to that for the corresponding elastic material. The axial pseudostrain is defined by:

$$\varepsilon_1^R(t) = \frac{1}{E_R}\int_{0^-}^{t} E(t-\tau)\frac{d\varepsilon_1^T(\tau)}{d\tau}d\tau \tag{15}$$

where $\varepsilon_1^R(t)$ is the axial pseudostrain; $\varepsilon_1^T(\tau)$ is the axial total strain measured in the test; $E(t)$ is the relaxation modulus of the undamaged material; and E_R is a reference modulus. Then the constitutive equation becomes:

$$\sigma(t) = E_R\varepsilon_1^R(t) \tag{16}$$

where $\sigma(t)$ is the stress as a function of time t. The purpose of using the E-VE correspondence principle is to eliminate the viscous effect on the material responses during both the damaged and undamaged behavior of the viscoelastic material. In fact, the EVCP was demonstrated to be valid not only in the condition with small deformation (e.g., linear viscoelastic material) but in the condition with large deformation (e.g., nonlinear viscoelastic with damage) (Schapery 1984; Kim et

al. 1995).The authors have demonstrated (Zhang, et al., 2012a) that the pseudostrain has a physical meaning provided that the reference modulus is the Young's modulus (i.e., $E_R = E_Y$). The physical meaning is that the pseudo-strain is the difference between the total strain and the viscous strain (i.e., $\varepsilon_1^R = \varepsilon_1^T - \varepsilon_1^{ve}$). In addition, the authors have demonstrated that the dynamic modulus at the critical nonlinear viscoelastic state is a good candidate for the reference modulus (Luo et al. 2013b, c, d; 2014b). A representative elastic modulus defined using the dynamic modulus master curve and relaxation modulus (i.e. $E_{re} = \frac{1}{2}\left[\left|E^*\right|_{f=\frac{1}{t_p}} + E\left(t = \frac{t_p}{2}\right)\right]$, t_p is the pulse time of a load) is proven to be equivalent to the dynamic modulus at the critical nonlinear viscoelastic state (Luo et al. 2016). In this way, the reference modulus can be obtained from the readily available material properties in the pavement design.

The E-VE correspondence principle was extended by the authors (Zhang et al. 2014c) to the three-dimensional condition for a viscoelastic material. The axial total strain and the radial pseudostrain are related as follows:

$$\varepsilon_1^T(t) = -\frac{1}{\upsilon_{12}^R}\varepsilon_2^R(t) \tag{17}$$

where υ_{12}^R is the reference Poisson's ratio that is assigned as the elastic Poisson's ratio (i.e., $\upsilon_{12}^R = \upsilon_0$). $\varepsilon_2^R(t)$ is the radial pseudostrain that is calculated by:

$$\varepsilon_2^R(t) = -\upsilon_{12}^R\left[-\int_{0^-}^{t}\pi_{12}(t-\tau)\frac{d\varepsilon_2^T(\tau)}{d\tau}d\tau\right] \tag{18}$$

where $\varepsilon_2^T(\tau)$ is the radial total strain that is measured in the test and $\pi_{12}(t)$ is the viscoelastic Poisson's ratio of the undamaged viscoelastic material. They are used together in the three dimensional EVCP and can characterize the linear viscoelastic materials under different loading conditions, e.g., strain decompositions and damage characterization in axial and radial directions.

4.4 Pseudostrain Energy

Pseudostrain defined in Equation 16 can be used to eliminate the time-dependent viscoelastic behavior from the damage within the material during the RDT test. Figure 6a presents a typical stress-strain and stress-pseudostrain hysteresis loop of asphalt mixture specimens in the

nondestructive RDT test. The area of the stress-strain and stress-pseudostrain hysteresis loops represent the amount of dissipated strain energy (DSE) and dissipated pseudostrain energy (DPSE) in the same load cycle, respectively. The figure shows that the stress-pseudostrain hysteresis loop follows a straight line in the nondestructive test, in which no damage is done and DPSE equals to zero. In the nondestructive test, all of the DSE is used for overcoming the viscoelastic resistance of the material. When the asphalt mixture is tested destructively, the DSE loop becomes larger because it is used for overcoming the viscoelastic resistance and inducing damage to the material. As a result, the stress-pseudostrain hysteresis loop is no longer a straight line. One pair of typical stress-strain and stress-pseudostrain hysteresis loops of asphalt mixtures in the destructive RDT test is shown in Figure 6b. The enclosed area of the stress-pseudostrain hysteresis loop represents the DPSE, which is consumed for cracking and permanent deformation in the asphalt mixture.

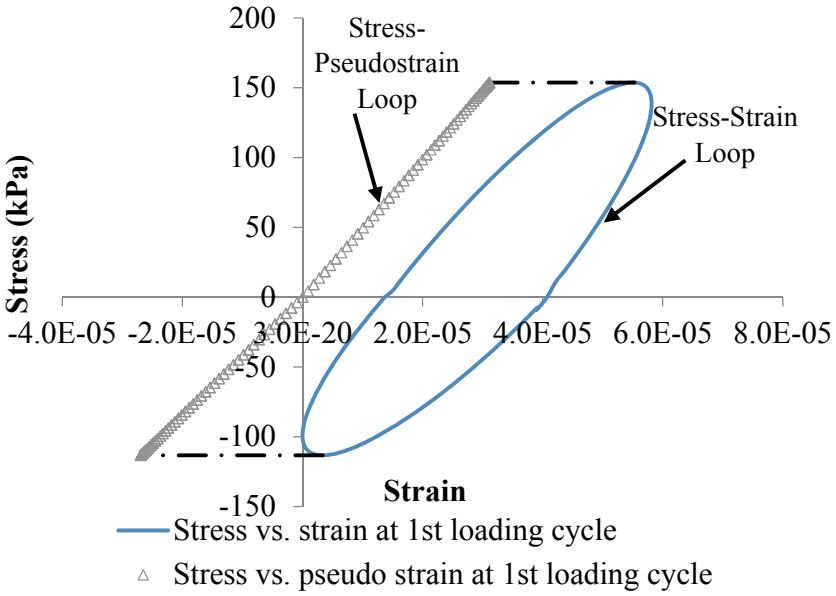

a. Hysteresis loop of an asphalt mixture specimen in nondestructive RDT test

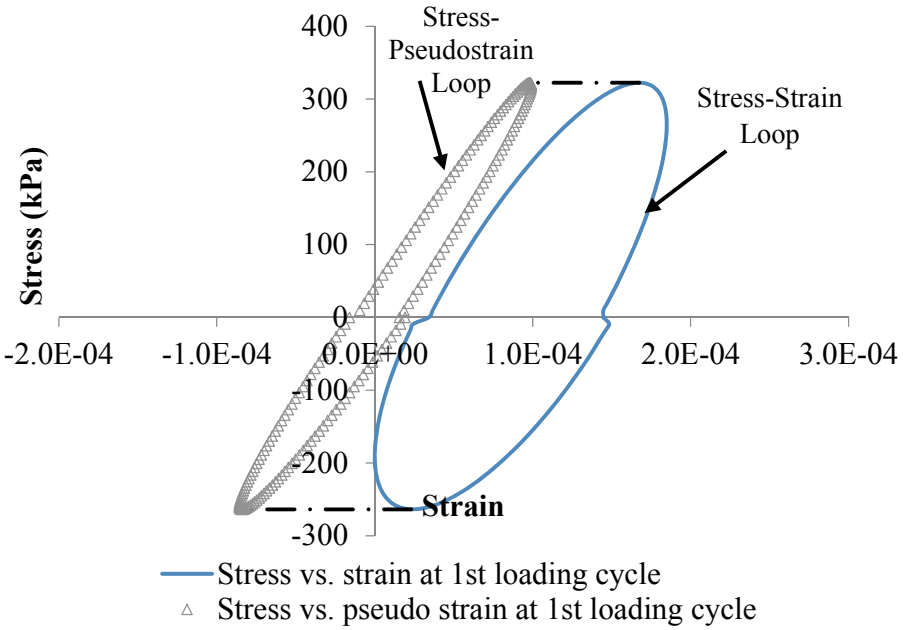

b. Hysteresis loop of an asphalt mixture specimen in destructive RDT test

Figure 6. Typical stress-strain and stress-pseudostrain hysteresis loops of asphalt mixtures in RDT test

The pseudostrain energy density (energy per unit volume) is calculated by integrating the stress and pseudostrain, which is presented in Equation 19.

$$W_R = \int_{t_1}^{t_2} \sigma(t) \frac{d\varepsilon_R(t)}{dt} dt \quad (19)$$

where W_R is the pseudostrain energy density in a loading period [t_1, t_2], $\sigma(t)$ is the time-dependent stress, and $\varepsilon_R(t)$ is the time-dependent pseudostrain. As illustrated in Figure 7, there are two types of pseudostrain energy. One is the DPSE, which is defined as the energy dissipated to develop damage in the specimen. The other is the recoverable pseudostrain energy (RPSE), which is stored and recovered with each load cycle in the material. The comprehensive equations and procedures for calculating the DPSE and RPSE are detailed in Luo et al. (2013b).

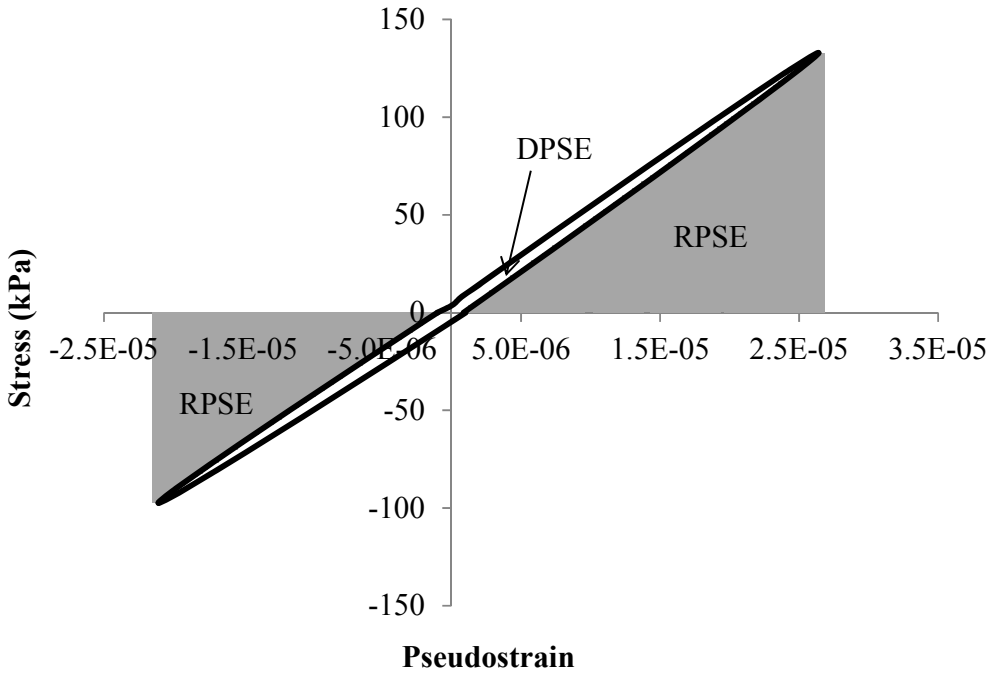

Figure 7. Illustration of DPSE and RPSE using stress-pseudostrain hysteresis loop

4.5 Strain Decomposition in Compression

Pseudostrain defined in Equation 16 can also be employed to perform strain decomposition. Both the total axial strain and radial strain measured in the destructive tests are decomposed into five components:

$$\varepsilon_i^T = \varepsilon_i^e + \varepsilon_i^p + \varepsilon_i^{ve} + \varepsilon_i^{vp} + \varepsilon_i^{vf} \tag{20}$$

where $i = 1, 2$ and $i = 1$ stands for axial variable and $i = 2$ stands for radial variable; ε_i^T is total strain; ε_i^e is elastic (instantaneous) strain; ε_i^{ve} is viscoelastic strain; ε_i^p is plastic strain; ε_i^{vp} is viscoplastic strain; and ε_i^{vf} is the viscofracture strain that is caused by growth of cracks (that exists only in the tertiary stage of a repeated load test in compression). The decomposition theory employs Hooke's law for the elastic strain in a small strain condition. The viscoelastic strain is substantially derived from linear viscoelastic theory that is the basis of the EVCP. The extra strains are caused by the development of irrecoverable deformations, which generate dissipated energy for viscoplasticity and fracture. The anisotropic strain decompositions can be accomplished by the following steps:

1) Elastic strains are calculated by the Hooke's law:

$$\begin{cases} \varepsilon_1^e = \sigma(t)/E_Y \\ \varepsilon_2^e = -\upsilon_0 \varepsilon_1^e \end{cases} \quad (21)$$

According to the EVCP, the viscoelastic strains are computed by subtracting the pseudostrain from the measured total strains:

$$\varepsilon_i^{ve} = \varepsilon_i^T - \varepsilon_i^R \quad (22)$$

2) At the instantaneous moment of loading, the viscoplastic and viscofracture strains do not occur since they are time-dependent variables, which means $\varepsilon_i^{vp}(t=0) = \varepsilon_i^{vf}(t=0) = 0$. Thus the instantaneous pseudostrain ($\varepsilon_i^R(t=0)$) is the sum of the plastic strain and the elastic strain. Therefore, the plastic strain can be calculated as:

$$\varepsilon_i^p = \varepsilon_i^R(t=0) - \varepsilon_i^e \quad (23)$$

3) The viscofracture strains are caused by the growth of cracks and they do not occur until the tertiary stage in a repeated load test in compression. This is due to a fact that the phase angle remains unchanged until the tertiary stage when cracks begin to grow. Thus, the viscoplastic strains in the primary and secondary stages ($\varepsilon_i^R(I, II)$) can be calculated by subtracting the elastic strains and the plastic strains from the calculated pseudostrain.

$$\varepsilon_i^{vp}(I, II) = \varepsilon_i^R(I, II) - \left(\varepsilon_i^e + \varepsilon_i^p\right) \quad (24)$$

The viscoplastic strain in the secondary and tertiary stages is then modelled by Tseng-Lytton model (Tseng and Lytton, 1989). Thus, the viscoplastic properties of the mixture, ρ and λ, are found in the secondary stage, prior to the onset of viscofracture. Then Equation 25 is used to predict the viscoplastic strain in the tertiary stage.

$$\varepsilon_i^{vp} = \varepsilon_{i\infty}^{vp} \exp\left[-\left(\rho_i/N\right)^{\lambda_i}\right] \quad (25)$$

4) Viscofracture strains are determined by subtracting all of the other strain components from the measured total strains.

$$\varepsilon_i^{vf} = \varepsilon_i^R - \left(\varepsilon_i^e + \varepsilon_i^p\right) - \varepsilon_i^{vp} \quad (26)$$

Figure 8 presents the results of the axial strain decomposition of an asphalt mixture. It is shown that the elastic and plastic strains are time-independent and the viscoelastic strains are present in all three stage changes and occupy a large proportion of the total strains. In addition, the viscoplastic strains follow the power curve in Equation 25. The viscofracture strains remain zero in the primary and secondary stages and increase with the increase of the number load cycles in the tertiary stage at an increasing strain rate. The decomposed viscoplastic and viscofracture strains

characterize the permanent deformation and crack growth of the asphalt mixture in compression, respectively. The number of load cycles of the initiation of the tertiary stage is the "Flow Number".

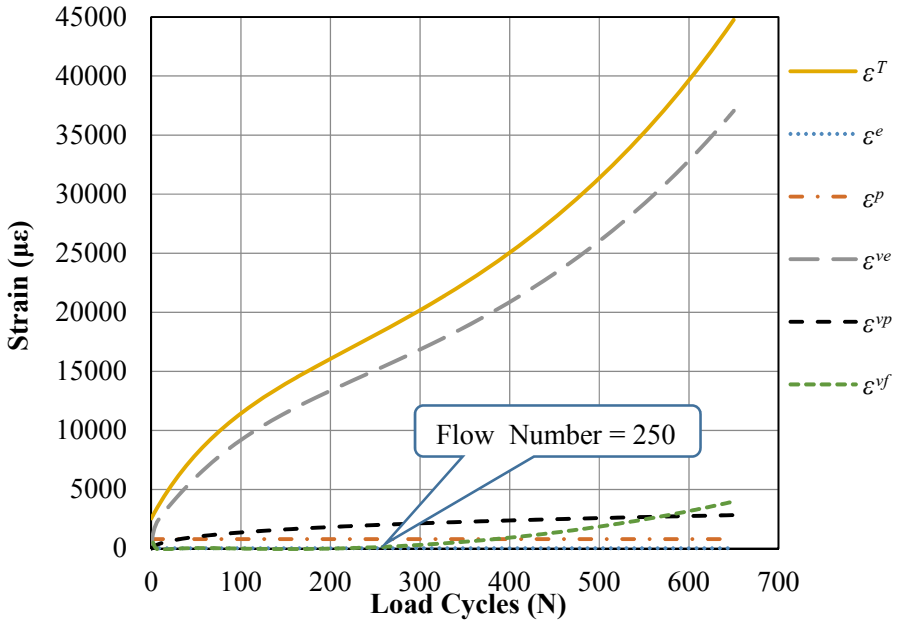

(a) Total strain and all strain components

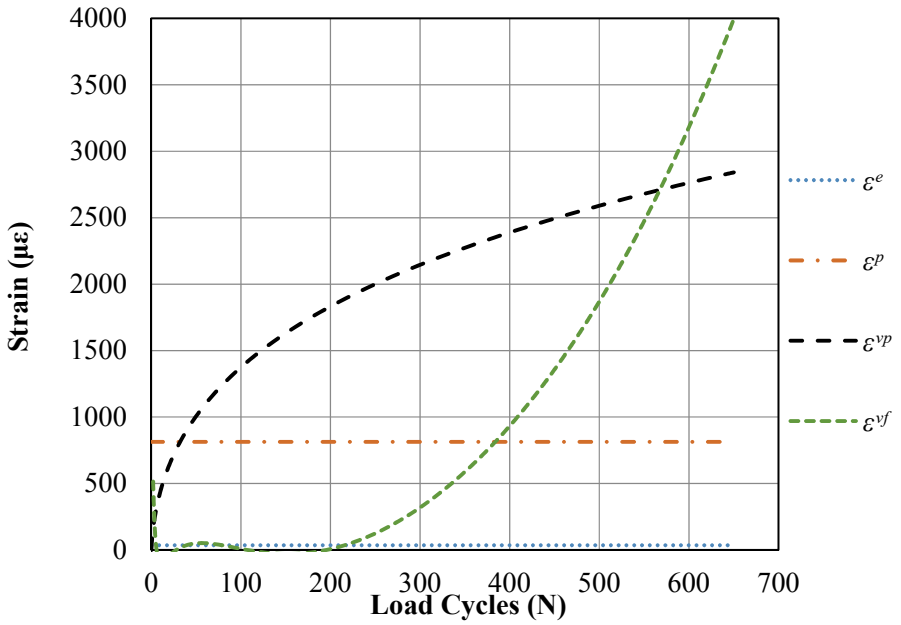

(b) Elastic, plastic, viscoplastic and viscofracture strain components

Figure 8. Strain decomposition in destructive dynamic modulus test for an asphalt mixture

5. Test Method and Typical Undamaged Properties of Asphalt Mixtures

5.1 Test Methods

To characterize the viscoelastic properties of undamaged asphalt mixtures, the nondestructive tests are employed to avoid the appearance of any damages. The criterion for separating the undamaged and damaged asphalt mixtures can be determined based on the change of dynamic modulus and phase angle with loading time or loading cycles as discussed in the previous section. These correspond to the initial yield stress in compression and endurance limit in tension, which are also temperature and loading rate dependent. For an unknown asphalt mixture, a rule of thumb which can be used in trial tests is to limit the total strain within 200 microstrains in compression and 70 microstrains in tension.

Asphalt mixture is anisotropic in compression and isotropic in tension. In addition, the uniaxial properties in compression differ from those in tension. Thus the fundamental viscoelastic material properties for an asphalt mixture should include the seven variables listed below:

1) compressive complex modulus in the vertical direction $E_{11}^{C*}(\omega)$;
2) compressive complex Poisson's ratio in the vertical plane $\nu_{12}^{C*}(\omega)$;
3) compressive complex modulus in the horizontal direction $E_{22}^{C*}(\omega)$;
4) compressive complex Poisson's ratio in the horizontal plane $\nu_{23}^{C*}(\omega)$;
5) compressive complex shear modulus in the vertical plane $G_{12}^{C*}(\omega)$;
6) tensile complex modulus $E_{11}^{T*}(\omega)$; and
7) tensile complex Poisson's ratio $\nu_{12}^{T*}(\omega)$.

In order to measure these properties simply, accurately, and rapidly, the authors recommend the use of three creep tests (uniaxial compressive creep, uniaxial tensile creep, and indirect tensile creep tests as shown in Table 1) at various temperatures. The stress and strain responses are measured in the creep tests including both vertical and horizontal strains, where the horizontal strains were measured using a bracelet mounted with a LVDT, as shown in the paper (Zhang et al. 2012b). These responses are used in the Laplace Transform Equations 13 and 14 to determine the time or frequency dependent material properties. For each complex property, the master curves of

its magnitude and phase angle are obtained for a complete characterization, which can be converted into the time domain properties such as relaxation modulus or creep compliance.

Table 1. Summary of Testing Protocols, Material Properties and Calculation Models for Characterizing the Undamaged Asphalt Mixtures (Zhang et al 2011, 2012b)

Test Method	Testing Parameters	Complex Parameters	Calculation Model
Uniaxial Compressive Creep Test	Testing: ▪ Constant compressive load σ_{11}^{C}; ▪ Test 60 seconds; ▪ Five temperatures: 10°C, 25°C, 40°C; Measured: ▪ Vertical strain ε_{11}^{C}; ▪ Horizontal strain ε_{22}^{C}.	Compressive Complex Modulus in Axial Direction $E_{11}^{C*}(\omega)$	$E_{11}^{C*}(\omega)=\left\{s\cdot\bar{E}_{11}^{C}(s)\right\}_{s=i\omega}=\left\{\frac{\bar{\sigma}_{11}^{C}(s)}{\bar{\varepsilon}_{11}^{C}(s)}\right\}_{s=i\omega}$
		Compressive Complex Poisson's Ratio in Axial Plane $\nu_{12}^{C*}(\omega)$	$\upsilon_{12}^{C*}(\omega)=\left\{s\cdot\bar{\nu}_{12}^{C}(s)\right\}_{s=i\omega}=\left\{-\frac{\bar{\varepsilon}_{22}^{C}(s)}{\bar{\varepsilon}_{11}^{C}(s)}\right\}_{s=i\omega}$
Uniaxial Tensile Creep Test	Testing: ▪ Constant tensile load σ_{11}^{T}; ▪ Test 60 seconds; ▪ Five temperatures: 0°C, 10°C, 25°C, 40°C; Measured: ▪ Vertical strain ε_{11}^{T}; ▪ Horizontal strain ε_{22}^{T}.	Tensile Complex Modulus in Axial Direction $E_{11}^{T*}(\omega)$	$E_{11}^{T*}(\omega)=\left\{s\cdot\bar{E}_{11}^{T}(s)\right\}_{s=i\omega}=\left\{\frac{\bar{\sigma}_{11}^{T}(s)}{\bar{\varepsilon}_{11}^{T}(s)}\right\}_{s=i\omega}$
		Tensile Complex Poisson's Ratio in Axial Plane $\nu_{12}^{T*}(\omega)$	$\upsilon_{12}^{T*}(\omega)=\left\{s\cdot\bar{\nu}_{12}^{T}(s)\right\}_{s=i\omega}=\left\{-\frac{\bar{\varepsilon}_{22}^{T}(s)}{\bar{\varepsilon}_{11}^{T}(s)}\right\}_{s=i\omega}$
Indirect Tensile Creep Test	Testing: ▪ Constant compressive load P; ▪ Test 60 seconds; ▪ Five temperatures: 10°C, 25°C, 40°C; Measured: ▪ Vertical compressive deformation U_3;	Compressive Complex Modulus in Radial Direction $E_{22}^{C*}(\omega)$	$E_{22}^{C*}(\omega)=\left\{s\cdot\bar{E}_{22}^{C}(s)\right\}_{s=i\omega}$ Eq. 65 of Zhang et al. (2012b)
		Compressive Complex Poisson's Ratio in Horizontal Plane $\nu_{23}^{C*}(\omega)$	$\nu_{23}^{C*}(\omega)=\left\{s\cdot\bar{\nu}_{23}^{C}(s)\right\}_{s=i\omega}$ Eq. 66 of Zhang et al. (2012b)

A creep test is much simpler and time-saving compared to dynamic modulus tests. The total loading time is limited to be within 1 minute for each creep test to keep the total strain within the undamaged strain criterion. Because of this, one day is sufficient to complete all of the above tests

for one sample including the tests at various temperatures. The frequency (in rad/sec) corresponding to the creep loading time is derived as $\omega = 1/2t$, where t is creep time in sec (Findley et al. 1989). Using this relationship, the complex modulus calculated from creep test data are demonstrated to be comparable to that measured directly with dynamic modulus tests (Zhang et al. 2012b).

5.2 Typical Results of Undamaged Asphalt Mixtures

Figure 9 plots the master curves of $\left|E_{11}^{C*}\right|$, $\left|E_{11}^{T*}\right|$ and $\left|E_{22}^{C*}\right|$, which are the material properties of a typical asphalt mixture. Each master curve has an S-shaped curve on the log scale of frequency. The magnitude of the radial compression modulus is always smaller than that of the axial compressive modulus. The magnitude of the tensile modulus is smaller than that of the compressive modulus but is much closer to the axial modulus at the higher loading frequencies. Figure 10 shows the master curves of $\varphi_{E_{11}^{C*}}$, $\varphi_{E_{11}^{T*}}$ and $\varphi_{E_{22}^{C*}}$, which are non-symmetric bell-shaped curves on the log scale of frequency. The tensile complex modulus shows a significantly larger phase angle than the compressive complex moduli at any given frequency This is because asphalt binder or mastic carries the tensile load when in tension; therefore the material has a more viscous response, which leads to a larger phase angle. In contrast, when the asphalt mixture is in compression, it is the aggregates interacting with the mastic that carries the compressive load, leading to a less viscous response and a smaller phase angle.

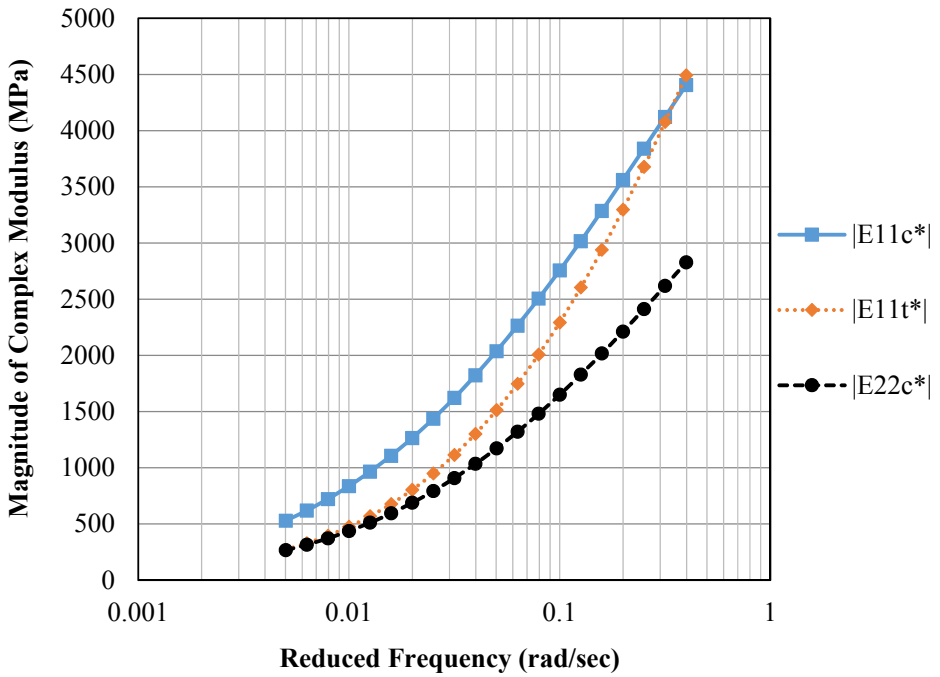

Figure 9. Master curves for the magnitude of E_{11}^{C*}, E_{11}^{T*} and E_{22}^{C*} at 20°C

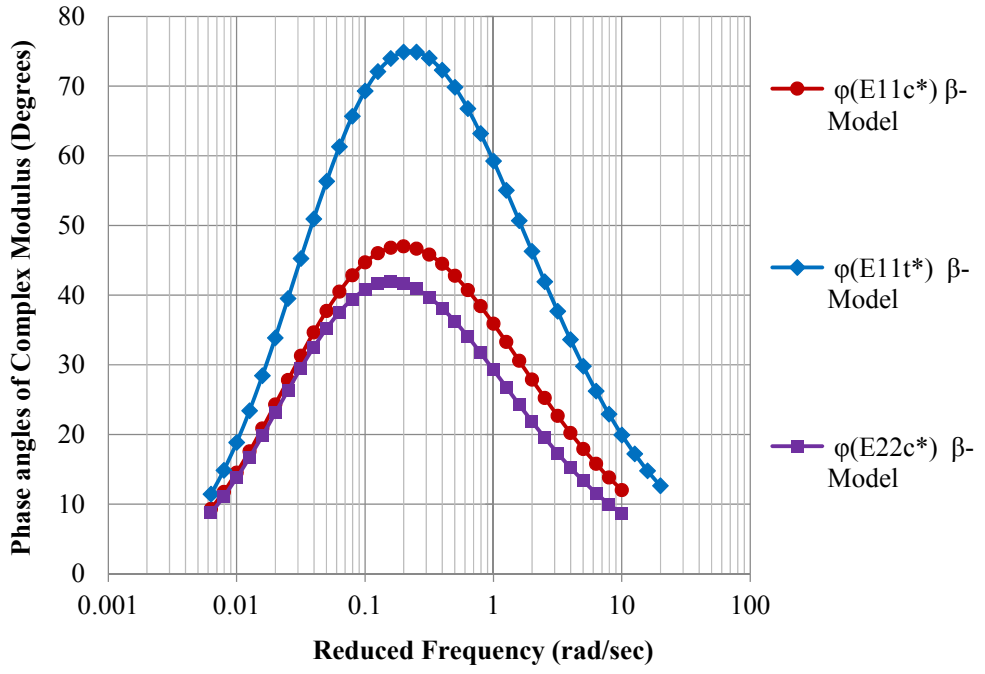

Figure 10. Master curves for the phase angles of E_{11}^{C*}, E_{11}^{T*} and E_{22}^{C*} at 20°C

Figures 11a and 11b show that the compressive and the tensile dynamic moduli both increase as the asphalt mixtures become stiffer due to aging or a smaller air void content. The phase angle decreases as the asphalt mixture is aged because the asphalt mixture behaves more elastically when it is aged. The phase angle has virtually no dependence on the air void content. Figure 11a also shows the Young's modulus and flow number determined from strain decomposition. The Young's modulus becomes larger and flow number increases when the material become stiffer due to lower air voids or being aged. All of the findings comply with the general understanding of the viscoelastic properties of asphalt mixtures. More test results including the model parameters for different asphalt mixtures can be found in Zhang (2012b)

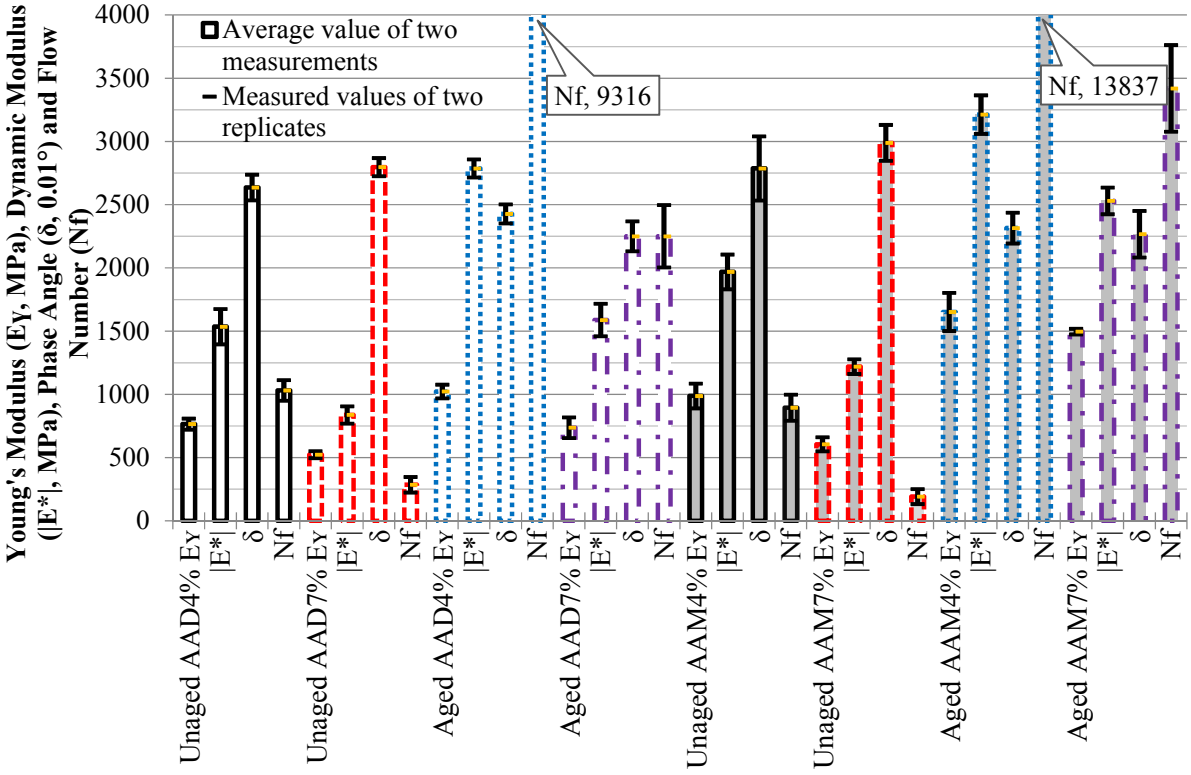

a. Young's modulus, dynamic modulus, phase angle (unit 0.01°) and flow number for different asphalt mixtures at 40°C, 1Hz in compression (the bar column represents the mean value of the two replicates)

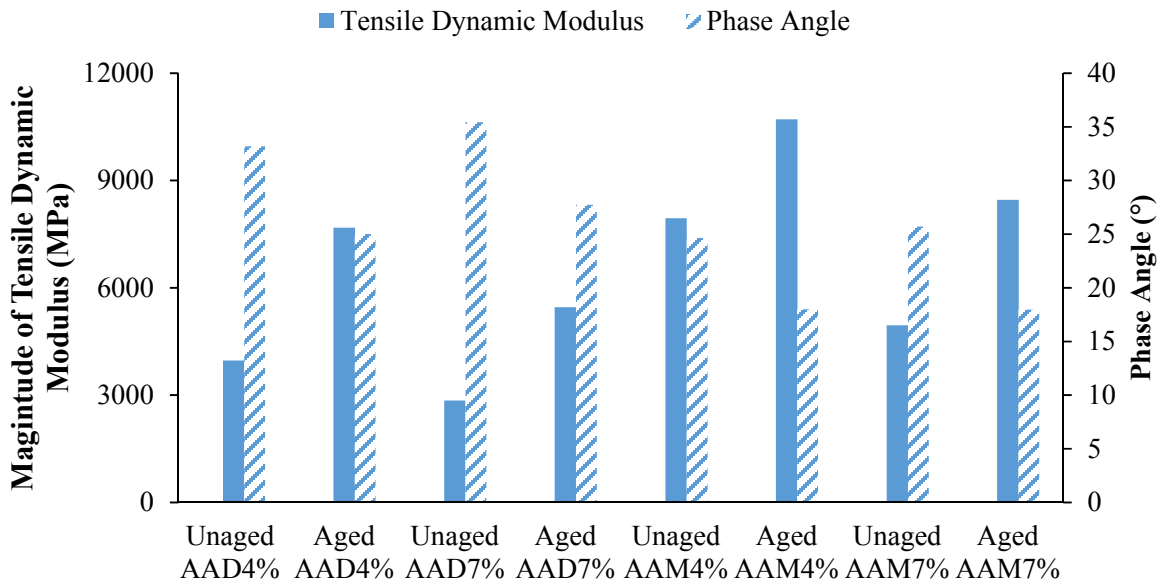

b. Dynamic modulus and phase angle for different asphalt mixtures at 20°C, 1Hz in tension

Figure 11. Effect of binder type, air void and aging on undamaged properties of asphalt mixtures

6. Effect of Aging on Undamaged Properties of Asphalt Mixtures

Aging refers to the process of change of chemical and physical properties of asphalt binder due to the oxidation and the loss of volatile oils, which significantly affects the undamaged properties of an asphalt mixture. Due to the non-uniform oxidation, the effect of aging varies with the depth below the surface of an asphalt pavement in the field. This produces a gradient of the complex modulus of the asphalt mixture which decreases with depth below the surface. A novel approach has been developed to predict the change of the modulus gradient due to in-service long term aging based on the aging kinetics (Luo et al. 2015). The modulus gradient in the field-aged asphalt mixtures is measured and calculated using the direct tension test (Koohi et al. 2012). Each field-aged asphalt mixture was cut into a rectangular specimen of 4 inches long, 3 inches wide and 1.5-2.5 inches thick. The specimen was glued with four pairs of linear variable differential transformers (LVDTs) to measure deformations at the top, center, and bottom of the asphalt layer. Then the specimen was subjected to a nondestructive monotonically increasing load at 10˚C and 20˚C, respectively. The elastic modulus of the tested specimen is modeled by:

$$E(z) = E_b + (E_s - E_b)\left(\frac{d-z}{d}\right)^n \tag{27}$$

where $E(z)$ is the elastic modulus at depth z; E_b and E_s are the elastic modulus at the bottom and top of an asphalt field core specimen, respectively; d is the thickness of the asphalt field core specimen; and n is the aging exponent that represents the shape of the modulus gradient with depth.

For each tested field core specimen, the elastic solution is converted to the viscoelastic solution using the elastic-viscoelastic correspondence principle. The major results include the complex bottom modulus, complex top modulus, and complex aging exponent. The magnitudes of the complex numbers refer to the dynamic bottom modulus $|E^*|_b$, dynamic surface modulus $|E^*|_s$, and the value of aging exponent is n. Figure 12 shows examples of the measured dynamic moduli of several field-aged foaming warm mix asphalt (FWMA) mixtures. As aging time increases, the magnitude of dynamic modulus within the top 1.5 inches increases and changes non-uniformly with the depth. It is also shown that the modulus gradient tends to be a vertical straight line as the depth increases below 1.5 inches. This indicates that the effect of aging on the mixture modulus is uniform at a depth below 1.5 inches. Based on the measured modulus gradient of field-aged asphalt mixtures, the modulus gradient in an asphalt pavement can be idealized as illustrated in Figure 13. The modulus at the 1.5-inch depth is the base-line modulus (i.e. $|E^*|_b$); the one at the surface is the surface modulus (i.e. $|E^*|_s$). The modulus gradient within the top 1.5-inch at any age is described by Equation 27; the modulus below the 1.5-inch depth is given by the base-line modulus.

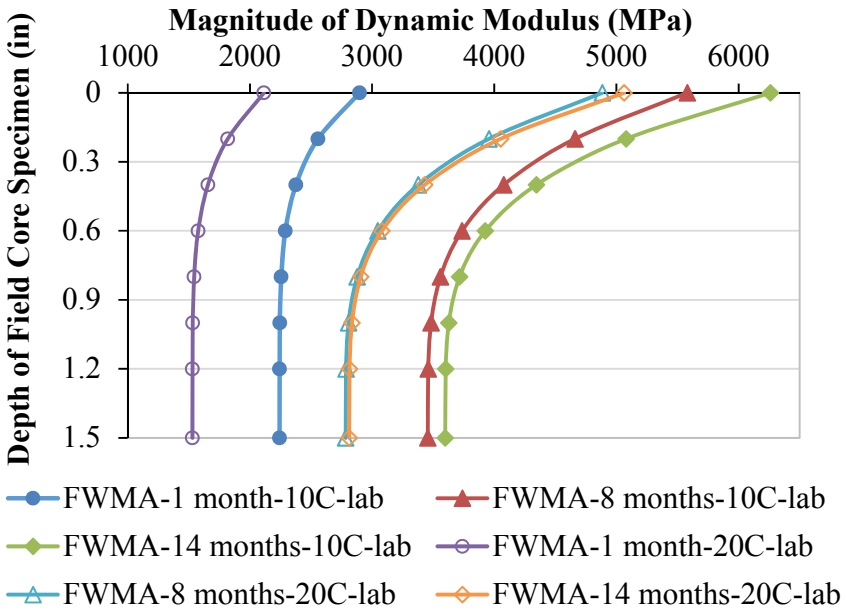

Figure 12. Laboratory measured modulus gradients in field-aged asphalt mixture

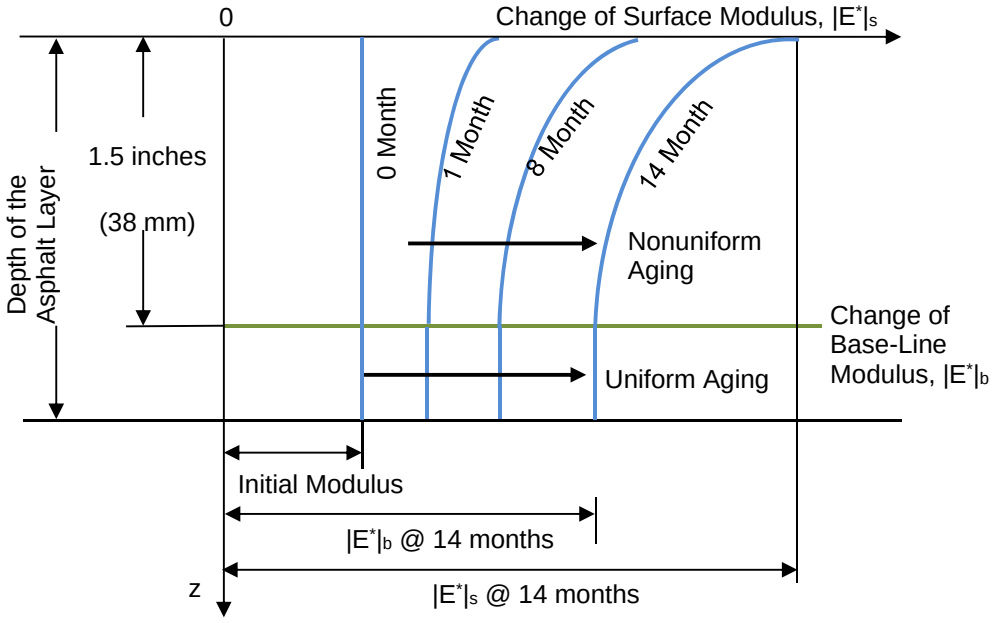

Figure 13. Idealization of modulus gradient in asphalt pavements

In order to predict the variation of the modulus gradient in an asphalt pavement with the aging time, aging models should be developed for the base-line modulus, surface modulus, and aging exponent, respectively. A two-stage kinetic aging model similar to the model that is used to predict the aging in asphalt binders (Jin et al. 2011) is used for this purpose. This mixture aging model predicts the evolution of the modulus gradient of an asphalt mixture with the aging time and temperature. The Arrhenius equation is employed to predict the variation of modulus with the temperature. A complete aging prediction model for the modulus gradient consists of three submodels to define how the magnitude of base-line modulus, surface modulus, and aging exponent change with the aging time, which are formulated as follows:

- Base-line modulus aging submodel:

$$\left|E^*\right|_b = \left|E^*\right|_{bi} + \left(\left|E^*\right|_{b0} - \left|E^*\right|_{bi}\right)\left(1 - e^{-k_{fb}t}\right) + k_{cb}t \tag{28}$$

in which $$k_{fb} = A_{fb}e^{-\frac{E_{afb}}{RT_{field}}} \tag{19}$$

$$k_{cb} = A_{cb}e^{-\frac{E_{acb}}{RT_{field}}} \tag{20}$$

- Surface modulus aging submodel:

$$\left|E^*\right|_s = \left|E^*\right|_{si} + \left(\left|E^*\right|_{s0} - \left|E^*\right|_{si}\right)\left(1 - e^{-k_{fs}t}\right) + k_{cs}t \tag{31}$$

in which: $k_{fs} = A_{fs} e^{-\frac{E_{afs}}{RT_{field}}}$ (32)

$$k_{cs} = A_{cs} e^{-\frac{E_{acs}}{RT_{field}}} \quad (33)$$

- Aging exponent submodel:

$$n = n_i - (n_i - n_0)\left(1 - e^{-k_{fn}t}\right) - k_{cn}t \quad (34)$$

in which: $k_{fn} = A_{fn} e^{-\frac{E_{afn}}{RT_{field}}}$ (35)

$$k_{cn} = A_{cn} e^{-\frac{E_{acn}}{RT_{field}}} \quad (36)$$

where $|E^*|_b$ and $|E^*|_s$ = the magnitude of the base-line modulus and surface modulus, respectively; $|E^*|_{bi}$ and $|E^*|_{si}$ = the initial magnitude of the base-line modulus and initial surface modulus, respectively; $|E^*|_{b0}$ and $|E^*|_{s0}$ = the intercept of the magnitude of the constant-rate line of the base-line modulus and that of the surface modulus, respectively; n_i = the initial magnitude of the aging exponent; n_0 = the intercept of the magnitude of the constant-rate line of the aging exponent; k_{fb}, k_{fs}, k_{fn} = the fast-rate reaction exponent for base-line modulus, surface modulus, and aging exponent, respectively; k_{cb}, k_{cs}, k_{cn} = the constant-rate reaction coefficient for base-line modulus, surface modulus, and aging exponent, respectively; t = the aging time in days; A_{fb}, A_{fs}, A_{fn} = the fast-rate pre-exponential factor for the base-line modulus, surface modulus, and aging exponent, respectively; E_{afb}, E_{afs}, E_{afn} = the fast-rate aging activation energy for the base-line modulus, surface modulus, and aging exponent, respectively; A_{cb}, A_{cs}, A_{cn} = the constant-rate pre-exponential factor for the base-line modulus, surface modulus, and aging exponent, respectively; E_{acb}, E_{acs}, E_{acn} = the constant-rate aging activation energy for the base-line modulus, surface modulus, and aging exponent, respectively; and T_{field} = the harmonic mean of the field aging absolute temperature. Equations 28 to 36 form a complete aging prediction model to predict the modulus gradient of field-aged asphalt mixture. The methodology to determine the parameters in these equations is detailed in Luo et al. (2015).

7. Summary

This study has summarized with examples the approach to determine the material properties of asphalt mixtures in an undamaged condition. The approaches to testing and analysis of the test data is focused on generating these material properties simply, rapidly and accurately with commonly available testing equipment. The approach can produce a complete characterization of the material properties of an asphalt mixture, both undamaged and damaged, in the course of one day.

A complete characterization includes the master curves of the magnitudes of the complex moduli and complex Poisson's ratios and their phase angles of the mixture in tension and compression as functions of frequency. A complete characterization also includes the material properties related to the viscoplasticity, viscofracture and healing of the mixture, but the measurement and analysis of these properties are treated in the next study. Central to being able to produce these properties so quickly and accurately are the use of the following concepts:

- Use of the elastic-viscoelastic correspondence principle and creep or monotonic loading to produce frequency-dependent properties of the mixture.
- Comprehensive use of the concept of pseudo-strain and its application in the decomposition of the measured strain into its undamaged and damaged components in both tension and compression tests.
- Recognition that the complex moduli and phase angles in tension and compression are different and that the moduli in tension are isotropic and those in compression are anisotropic. The master curves of the phase angles of both the complex moduli and complex Poisson's ratios, when plotted against frequency, are bell-shaped and non-symmetric.
- Consideration of the dependence of the material properties on in-service conditions like temperature, field aging, and pavement depth.

It is important to get these undamaged characterizations accurate because the determination of the damaged properties depend upon them being accurate. Using some other conveniently assumed property relation such as that the moduli and phase angles in tension and compression are the same or that the moduli in compression are isotropic introduce systematic errors in the predictions that are made with the assumed relations. The simplicity and accuracy of the test methods described in this study and the next one make these convenient assumptions unnecessary and avoid the possibly large systematic errors in the predictions that are made with the assumed properties.

The overall purpose of getting these material properties right is to be able to choose the materials to use in construction more wisely and to anticipate and plan for their eventual deterioration more accurately, thus making management feasible and a major reduction in the huge costs of deferred maintenance possible.

References

1. Arambula, E. (2007). "Influence of Fundamental Material Properties and Air Void Structure on Moisture Damage of Asphalt Mixes." Ph.D. Dissertation, Texas A&M University, College Station, Texas.
2. Carpenter, S. H., Ghuzlan, K. A., and Shen, S. (2003). "Fatigue Endurance Limit for Highway and Airport Pavements." *Transportation Research Record: Journal of the Transportation Research Board*, 1832(1), 131-138.
3. Findley, W. N., Lai, J. S., and Onaran, K. (1989). "Creep and Relaxation of Nonlinear Viscoelastic Materials with an Introduction to Linear Viscoelasticity." Dover Publication, Inc., Mineola, New York.
4. Gu, F., Zhang, Y., Luo, X., Luo, R., and Lytton, R. L. (2015a). "Improved Methodology to Evaluate Fracture Properties of Warm-mix Asphalt Using Overlay Test." *Transportation Research Record: Journal of the Transportation Research Board*, 2506(1), 8-18.
5. Gu, F., Luo, X., Zhang, Y., and Lytton, R. L. (2015b). "Using Overlay Test to Evaluate Fracture Properties of Field-aged Asphalt Concrete." *Construction and Building Materials*, 101(1), 1059-1068.
6. Jin, X., Han, R., Cui, Y., and Glover, C. J. (2011). "Fast-Rate-Constant-Rate Oxidation Kinetics Model for Asphalt Binders." *Industrial and Engineering Chemistry Research*, 50(23), 13373-13379.
7. Koohi, Y., Lawrence, J. J., Luo, R., and Lytton, R. L. (2012). "Complex Stiffness Gradient Estimation of Field-Aged Asphalt Concrete Layers Using the Direct Tension Test." *Journal of Materials in Civil Engineering*, American Society of Civil Engineers (ASCE), 24(7), 832-841.
8. Kim, Y. R., Lee, Y. C., and Lee, H. J. (1995). "Correspondence Principle for Characterization of Asphalt Concrete." *Journal of Materials in Civil Engineering*, American Society of Civil Engineers (ASCE), 7(1), 59-68.
9. Luo, R., and Lytton, R. L. (2010). "Characterization of the Tensile Viscoelastic Properties of an Undamaged Asphalt Mixture." *Journal of Materials in Civil Engineering*, American Society of Civil Engineers (ASCE), 136(3), 173-180.
10. Luo, X., Luo, R., and Lytton, R. L. (2013a). "Characterization of Asphalt Mixtures Using Controlled-Strain Repeated Direct Tension Test." *Journal of Materials in Civil Engineering*, American Society of Civil Engineers (ASCE), 25(2), 194-207.

11. Luo, X., Luo, R., and Lytton, R. L. (2013b). "Characterization of Fatigue Damage in Asphalt Mixtures Using Pseudostrain Energy." *Journal of Materials in Civil Engineering*, American Society of Civil Engineers (ASCE), 25(2), 208-218.
12. Luo, X., Luo, R., and Lytton, R. L. (2013c). "Energy-Based Mechanistic Approach to Characterize Crack Growth of Asphalt Mixtures." *Journal of Materials in Civil Engineering*, 25(9), 1198-1208.
13. Luo, X., Luo, R., and Lytton, R. L. (2013d). "Modified Paris' Law to Predict Entire Crack Growth in Asphalt Mixtures." *Transportation Research Record: Journal of the Transportation Research Board*, 2373, 54–62.
14. Luo, X., Luo, R., and Lytton, R. L. (2014a). "Energy-Based Crack Initiation Criterion for Visco-Elasto-Plastic Materials with Distributed Cracks." *Journal of Engineering Mechanics*, 141(2), p. 04014114.
15. Luo, X., Luo, R., and Lytton, R. L. (2014b). "Energy-Based Mechanistic Approach for Damage Characterization of Pre-Flawed Visco-Elasto-Plastic Materials." *Mechanics of Materials*, 70, 18-32.
16. Luo, X., Gu, F., and Lytton, R. L. (2015). "Prediction of Field Aging Gradient in Asphalt Pavements." *Transportation Research Record: Journal of the Transportation Research Board*, 2507(1), 19-28.
17. Luo, X., Zhang, Y., and Lytton, R. L. (2016). "Implementation of Pseudo J-Integral Based Paris' Law for Fatigue Cracking in Asphalt Mixtures and Pavements." *Materials and Structures*, 49(9), 3713-3732.
18. Marasteanu, M. O., and D.A. Anderson. (1999). "Improved Model for Bitumen Rheological Characterization." *Eurobitume Workshop on Performance Related Properties for Bituminous Binders*, Luxembourg, Paper No. 133.
19. Park, S. W., and Schapery, R. A. (1999). "Methods of Interconversion between Linear Viscoelastic Material Functions. Part I-A Numerical Method Based on Prony Series." *International Journal of Solids and Structures*, 36(11), 1653-1675.
20. Schapery, R. A. (1984). "Correspondence Principles and a Generalized J-integral for Large Deformation and Fracture Analysis of Viscoelastic Media." *International Journal of Fracture*, 25(3), 195-223.
21. Si, Z. (2001). "Characterization of Microdamage and Healing of Asphalt Concrete Mixtures."

Ph.D. Dissertation, Texas A&M University, College Station, Texas.

22. Wineman, A. S., and Rajagopal, K. R. (2001). “Mechanical Response of Polymers, an Introduction.” Cambridge University Press, New York.
23. Witczak, M., Mamlouk, M., Souliman, M., and Zeiada, W. (2013). “Laboratory Validation of an Endurance Limit for Asphalt Pavements.” NCHRP report 762, National Cooperative Highway Research Program, Washington, DC.
24. Zhang, Y., Bernhardt, M., Biscontin, G., Luo, R., and Lytton, R. L. (2014a). "A Generalized Drucker-Prager Viscoplastic Yield Surface Model for Asphalt Concrete." *Materials and Structures*, Springer; 48(11), 3585-3601.
25. Zhang, Y., Luo, X., Luo, R., and Lytton, R. L. (2014b) "Crack Initiation in Asphalt Mixtures under External Compressive Loads." *Construction and Building Materials*, Elsevier; 72, 94-103.
26. Zhang, Y., Luo, R., and Lytton, R. L. (2014c). "Anisotropic Modeling of Compressive Crack Growth in Tertiary Flow of Asphalt Mixtures." *Journal of Engineering Mechanics*, American Society of Civil Engineers (ASCE), 140(6), 04014032.
27. Zhang, Y., Luo, R., and Lytton, R. L. (2013a). "Characterization of Viscoplastic Yielding of Asphalt Concrete." *Construction and Building Materials*, Elsevier, 47, 671-679.
28. Zhang, Y., Luo, R., and Lytton, R. L. (2013b). "Mechanistic Modeling of Fracture in Asphalt Mixtures under Compressive Loading." *Journal of Materials in Civil Engineering*, American Society of Civil Engineers (ASCE), 25(9), 1189-1197.
29. Zhang, Y., Luo, R., and Lytton, R. L. (2012a). "Characterizing Permanent Deformation and Fracture of Asphalt Mixtures by Using Compressive Dynamic Modulus Tests." *Journal of Materials in Civil Engineering*, American Society of Civil Engineers (ASCE), 24(7), 898-906.
30. Zhang, Y., Luo, R., and Lytton, R. L. (2012b). "Anisotropic Viscoelastic Properties of Undamaged Asphalt Mixtures." *Journal of Transportation Engineering*, American Society of Civil Engineers (ASCE), 138(1), 75-89.
31. Zhang, Y., Luo, R., and Lytton, R. L. (2011). "Microstructure-based Inherent Anisotropy of Asphalt Mixtures." *Journal of Materials in Civil Engineering*, American Society of Civil Engineers (ASCE), 23(10), 1473-1482.